Original Article

Assessing the Impact of Nano Silica and Nano Carbonate on High Strength Concrete Properties through Statistical Modelling

Chitturi Sravanti¹, P Srinivasa Rao²

^{1,2}Department of Civil Engineering, JNTUH University College of Engineering, Science & Technology, College of Engineering (Autonomous), Hyderabad, Telangana.

¹Corresponding Author: sravantichitturi9@gmail.com

Revised: 10 October 2025 Received: 09 September 2025 Accepted: 08 November 2025 Published: 29 November 2025

Abstract - The impact of Nano Silica (nS) and Nano Calcium Carbonate (nC) on the hardened and fresh attributes of M90 High Strength Concrete (HSC) is investigated in this work, Ordinary Portland Cement (OPC) 53 grade (65%), Fly Ash (15%), Micro Silica (10%), and Quartz Powder (10%) made up the binder system's total weight. Both nS and nC are added at dosages of 3% by weight of cement content to improve performance. The design mix (HSC 3nS 3nC) contained both nanomaterials, whereas the control mix (HSC 0nS 0nC) contained neither. With increasing nano content, the outcomes showed a slight decrease in workability; the slump decreased from 70 mm for the control mix to 51 mm for the highest nano addition. Nonetheless, notable advancements in mechanical characteristics are noted. In comparison to the control, which had a compressive strength of 115.31 MPa, the design mix increased from 102.71 MPa to 113.42 MPa at 28 days, reaching 131.68 MPa at 180 days. In a similar vein, the split tensile strength increased from 9.01 MPa to 9.98 MPa at 180 days and from 7.96 MPa to 8.57 MPa at 28 days. At 28 days, bending strength increased from 10.82 MPa to 11.64 MPa, and at 180 days, it increased from 12.15 MPa to 13.48 MPa. These results confirm that the long-term strength development of HSC is pointedly enhanced by the combined addition of nS and nC, providing better durability potential with a manageable loss of workability. A regression analysis is conducted to establish the correlation between mechanical strengths, revealing strong positive relationships among these properties. The efficacy of the empirical predicted equations presented by investigators and the anticipated equation is assessed by means of statistical parameters such as Root Mean Square Error (RMSE), Integral Absolute Error (IAE), Normal Efficiency (NEF), and Mean Absolute Error (MAE).

Keywords - High Strength Concrete, Nano Silica, Nano Calcium Carbonate, Ouartz Powder, Ouartz Sand.

1. Introduction

Concrete is the most broadly employed material in construction around the world. It is the dominant modern construction and infrastructure material due to its versatility, affordability, and ability to be adapted to various engineering applications [1]. Concrete is used for a variety of built forms and infrastructural projects, from tall buildings to wide bridge decks to large industrial structures; concrete is essential for shaping the built environment. Among the many types of concrete, High-Strength Concrete (HSC), defined as concrete having Compressive Strength (CS) over 60 MPa, has become more and more understood and utilized by design professionals over the last few decades. This evolution has been due to the increase in expectation for slender structural elements, long-span bridges, construction of heavier loading structures, and durable construction in potentially aggressive environments [2]. HSC allows for structurally efficient, less physically intrusive members, while providing resilience and performance that are subjected to extreme mechanical loading and environmental deterioration, thereby making it the material of choice in high-performance applications. Nevertheless, preparing HSC introduces several limitations. In contrast to traditional concrete, high CS in HSC can be achieved only through careful attention to the mix design, use of constituents, control of workability, and then consolidation of microstructure [3]. HSCs, though mechanically superior, are also more brittle and less ductile, and are sensitive to curing and microcrack propagation. Therefore, understanding the extent to which nano additives can assist in overcoming these durability-related issues in practical curing conditions is crucial for applicability. Traditional HSC mixes have emphasized high-quality binder materials, low (w/b < 0.40), and the practice of Supplementary Cementitious Materials (SCMs) like Fly Ash (FA), Microsilica (MS), and Quartz Powder (QP). SCMs are crucial because they improve the mechanical and durable qualities of the cement matrix by

reducing porosity, increasing packing density, and densifying the internal morphology. SCMs only have a limited impact on concrete's microscale characteristics, despite advancements [4]. Although SCMs decrease capillary porosity and encourage the addition of hydration products like Calcium Silicate Hydrate (C-S-H), they are unable to address the ITZ, which is the area between the aggregate and the cement paste and is typically the frailest link in the concrete as a whole. Microcracks are initiated by these weak ITZs and impact structural performance, chemical resistance, and longterm durability [5]. New directions in concrete science that provide alternate paths through conventional materials have been made possible by developments in nanotechnology. The hydration kinetics, microstructure development, mechanical attributes of cementitious systems can be meaningfully enhanced by nano-scale engineered materials like Nano-Silica (nS) and Nano-Calcium Carbonate (nC). Engineered nanomaterials' ultra-fine particle size and surface area enable them to fill in nanometric voids, react with hydration products more efficiently, and produce denser and more homogeneous microstructures [6]. nS is especially good at affecting the hydration process. It can be both a reactive pozzolan and a nucleation location for C-S-H gel creation. nS reduces the amount of reactive phase available for chemical attack by consuming Ca (OH)₂, improving the packing density of the cement paste.

This will result in decreased porosity, increased mechanical strength, and improved performance against aggressive environments. Not only will nS improve mechanical strength performance, it will accelerate early-age hydration, leading to higher strength development and better long-term performance [7]. In contrast, nano-calcium carbonate mainly acts as filler and crystallizer, functioning to allow the early hydration phase to occur more quickly by acting as a nucleation agent and increasing the speed of C-S-H creation by behaving as a nucleation agent. It is also small enough to fill micro- and nano-voids, mainly in the ITZ, which may improve bond strength and reduce permeability. It may also be able to buffer the alkalinity of the pore solution, which can reduce chemical degradation for aggressive environments [8]. While the repercussions of nS and nC on concrete performance have each been thoroughly researched, the interactions created by both nanomaterials when utilized in HSC systems have not been fully explored in existing research. These interactions may result in improved hydration kinetics, enhanced pore refinement, superior mechanical attributes, and more due to the use of both nanomaterials compared to the use of either individual nanomaterial, as well as any SCMs such as FA, MS, and/or QP. Some study results when using both nanomaterials (with or without SCMs) indicated an improvement in compressive and bending strength, while some studies also highlighted things like a loss in workability, agglomeration, and dispersion when utilizing two different nanomaterials simultaneously. As a result, thoroughly understanding all interactions of nano-silica, nanocalcium carbonate, and other SCMs is critically important to maximize HSC performance [9]. Quartz Sand (OS) as fine aggregate is another important ingredient of the HSC system examined in this study. QS is different from ordinary river sand or crushed sand in that it is highly angular with low porosity and high surface purity, hence offering advantages for packing density and mechanical properties. However, the interaction between OS and nanomaterial-modified cement paste has rarely been addressed. On one hand, the rigid and non-reactive surface of quartz particles could have an influence on the ITZ development, and, on the other hand, together with nanomaterials, it might result in unique microstructural improvements that benefit both fresh and hardened properties [10]. Even though a rising number of scholarly works have been conducted on the matter of nanomaterial-modified concrete, the literature still lacks studies on the comprehensive integration of multiple supplementary cementitious materials, nanomaterials, and special aggregates such as quartz sand into a single HSC system. Prior studies [6-10] show that nS aids hydration kinetics and nC accelerates nucleation at early ages, but most studies concentrate on single mechanical tests without consideration of statistical correlations or durability over time. Thus, an assessment of dual-nanomaterial-modified HSC is needed. Most investigations have dealt with isolated effects or limited combinations of materials, often without due regard to practical real-world constraints such as workability, setting time, and durability under an aggressive environment. Nevertheless, while there is substantial literature on single nanomaterials, insight into the synergistic effect of nS and nC with SCMs, as well as quartz aggregates, in HSC is limited. The current study attempts to fill the unexplored area by investigating the collective outcome of nS and nC on the fresh state and hardened attributes of concrete with M90 grade HSC.

The research is an extensive experimental study to comprehend the consequences of nS and nC on the fresh and hardened attributes of M90 grade HSC. The binder system is carefully designed using OPC 53 grade, FA, MS, and QP, with nS and nC added at 3% each by mass of cement for the improvement of performance. Workability (slump) and various mechanical strengths like compressive, split tensile, and bending are determined at 28, 56, 90, and 180 days of water curing. Apart from the mechanical properties, a regression analysis is also carried out to predict an empirical relationship between the strengths. The proposed equations enable the tensile and flexural behaviour to be predicted from CS data, which gives good significance in practical design and quality control. The originality of this study lies in the integrated investigation of dual nanomaterial modification (nS and nC) in a multi-component binder system (OPC, FA, MS, and QP). This is unlike previous studies that exclusively investigated isolated nano additives. This study statistically models the mechanical behaviour of HSC by identifying empirical relationships validated against international codes and literature, as a design tool for structural engineers.

2. Materials and Procedures

2.1. Binders

The binder system consists of OPC (65%) as the primary cementitious material and FA (15%), MS (10%), and QP (10%) by total weight of the binder contents. Two nanomaterials, nS and nC, are also used at 3% each by weight of cement content, to further improve performance. The final amounts are determined after several trial mixes that studied workability, CS, and setting times. It is determined that 3% each of nS and nC could be introduced without hindering the fresh property performance of the concrete. 53 grade OPC is used, which satisfies the IS: 12269 specifications that have a relative density of 3.15. Class F, FA is acquired from a local supplier, used to aid workability and its pozzolanic functions over the long term, and has a specific gravity of 2.20. MS is acquired from a manufacturer that is used as a highly reactive pozzolanic material, which densifies pore structure, and can strengthen ITZ, and has a specific gravity of 2.17. QP of size 10µm is used to advance the packing compactness of the particles in the binder matrix and can help compress air voids in the hardened paste, with a specific gravity of 2.60. nS of average particle size 17nm is supplied by a local supplier, which is highly pozzolanic, acting as a nucleating promoter C-S-H formation and significantly refining the microstructure, and its specific gravity is 2.20. nC of average particle size 30nm is sourced from a chemical supplier, acts more as a micro-filler, and a nucleation site, helping early hydration and better packing density.

The specific gravity of nC is 2.70. These binder components are proportioned as a multi-component mixture and combined to optimize the constituent components for HSC that will maximize mechanical performance and durability. Table 1 outlines a summary of the oxide composition of the binder sources. Figure 1 and 2 shows the XRD images of nS and nC.

2.2. Aggregates and Super Plasticizer

Quartz Sand (QS) served as the fine aggregate throughout the experimental work. QS used has a typical particle diameter of $100~\mu m$, alongside a relative density of 2.60. Given its silica content and the artificially angular shape of the particles, QS adds to the packing density of concrete and ultimately the strength potential in HSC. The coarse aggregate is crushed locally sourced granite, having a maximum size of 20~mm.

The coarse aggregate achieved a specific gravity of 2.65, a fineness modulus of 7.31, and a water absorption of 0.75% which allows for the appropriate corrections to the mix water content in the desired w/c of 0.23. Fosroc Conplast SP 430, a polycarboxylic ether-derived Super Plasticizer (SP), is used to improve the workability of the HSC without bleed or segregation. This SP is known to be highly dispersive and is compatible with nano-modified cementitious systems. It is used at 1.22% by weight of binder, which is identified from trial mixes to achieve the desired flow and cohesive behaviour. It has a specific gravity of 1.1 as per the manufacturer, making it a low-density admixture that can easily blend into the concrete matrix without compromising the density of the mix. Locally available tap water is used. Figure 3 shows all the materials used before mixing.

Table 1. Oxide composition of the binders

Oxide			(%	%)		
Oxide	OPC	FA	MS	QP	nS	пC
CaO	64	3.0	1.0	0.01	-	98.3
Al_2O_3	5.5	24	1.2	0.08	0.05	0.1
SiO_2	21	60.5	93.0	99.5	99.88	0.1
Fe ₂ O ₃	3.2	6.5	0.6	0.04	0.001	0.01
SO_3	2	0.5	0.2	-	-	-
MgO	2	1.2	0.3	0.01	0.01	0.16
Na ₂ O	0.2	0.8	0.5	-	0.04	0.16
K ₂ O	0.6	1.0	0.8	-	0.03	-

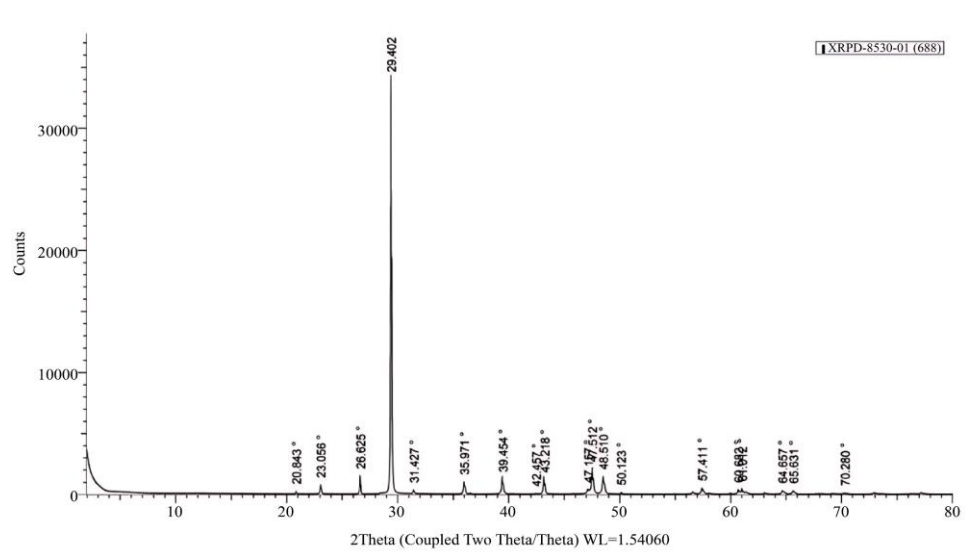


Fig. 1 X-Ray Diffraction output of nC

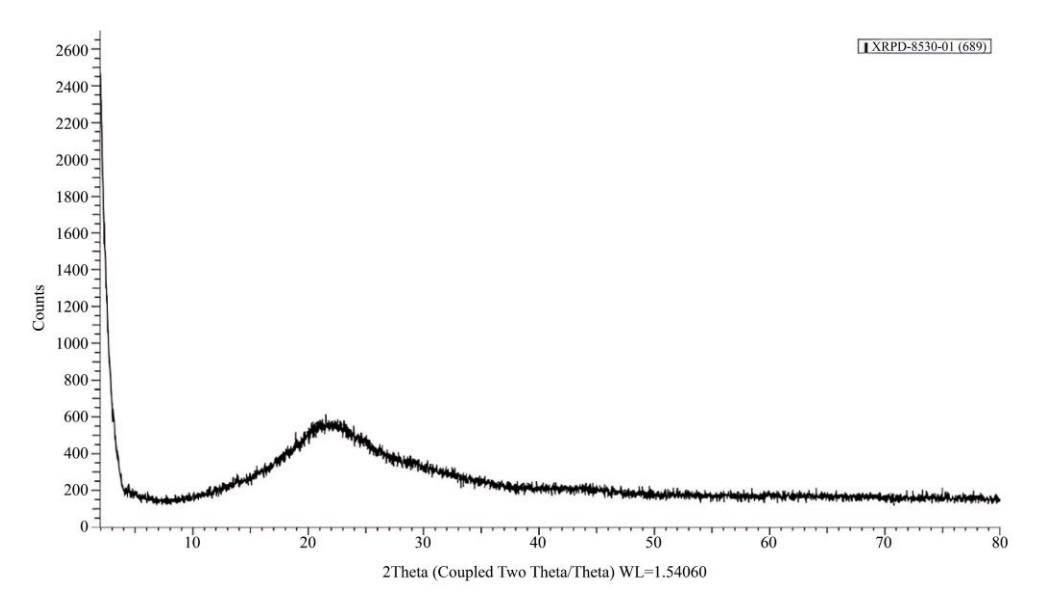


Fig. 2 X-Ray Diffraction output of nS



Fig. 3 Raw materials for HSC

2.3. Mix Design

M90 grade HSC is designed in accordance with IS 10262:2019. To achieve the overall objective of producing a concrete that meets a target strength in compression (CS) of 98.25 MPa at 28 days, numerous trial mixes are prepared by modifying the replacement level of nS and nC to reach an optimum dosage providing advantageous mechanical properties while not adversely impacting the workable nature of the fresh concrete. Grounded on the results of these trials, a replacement level of 3% nS and 3% nC (by mass of cement) is finally selected. Thus, the two distinct mixes are prepared: HSC 0nS 0nC, the control mix that contained no nano additives, and HSC 3nS 3nC, the design mix with 3% nS and

3% nC as partial replacements for the cement, maintaining the same ratios for the other binders and aggregates. Table 2 gives the mix design values (kg/m³). All concrete batches are produced via a pan mixer to distribute the nanomaterials within the binder matrix.

For HSC production, the cement, FA, MS, QP, nS, nC, and QS are dry blended for approximately 2 minutes, obtaining a homogeneous dry mix. The mixing water, which contained the specified mixing dose of SP, is gradually added, followed by the remaining water for final mixing that lasted for an additional 3-4 minutes, obtaining a uniform, workable, and cohesive mix that will cast and be tested.

Table 2. Mix Design of M90 HSC (kg/m³)

Mix Designation	OPC	FA	MS	QP	nS	nC	QS	Coarse Aggregate	SP
HSC 0nS 0nC	497	115	77	77	0	0	501	913	9.5
HSC 3nS 3nC	451	115	77	77	23	23	497	906	9.3

2.4. Methods

The fresh and hardened characteristics of the HSC mixes are assessed by the following laboratory tests. The slump test is carried out to assess workability by utilizing a standard slump cone according to IS 1199:2018 (Part 2). Fresh concrete is cast inside the cone, and after being raised straight up, the slump of the concrete is measured to assess consistency. For the mechanical strength tests (as per IS 516:2021 Part I, Section 1), CS is determined by testing 150 mm cube specimens after demoulding and then cured in water for the prescribed time, and then put under uniaxial compression on a Compressive Testing Machine until failure; once a failure occurred, the maximum load is recorded to ascertain strength. Split Tensile Strength (STS) is conducted on 150 mm diameter × 300 mm long cylindrical samples placed horizontally and then loaded diametrically until failure occurred, and assessed using the peak load at failure, and noted. Flexural Strength (FS) is determined with 100 mm \times 100 mm \times 500 mm prism samples placed on supporting rollers and loaded by means of a two-point loading; the ultimate load at failure is noted to determine FS. All tests are executed according to the provisions of the Indian Standards described above. All results presented are the mean of three specimens per condition for each test. For all mixes, specimens were tested immediately after mixing at a controlled temperature (27 ± 2 °C) and humidity (60 \pm 5 %). All mixes are cured in potable water at 27 °C to produce consistent hydration conditions for both the control and nano-modified mixes. Regression models are created using least-squares fitting in Microsoft Excel. RMSE, IAE, MAE, and NEF are used to evaluate the regression model, and dosages are adjusted using the iterative process to balance workability and CS.



Fig. 4 Measured Slump of HSC

3. Results and Discussions

3.1. Workable Nature

The HSC 0nS 0nC mix yielded a slump of 70 mm, and the design mix that contained 3% nS and 3% nC (HSC 3nS 3nC) yielded 51mm, as shown in Figure 4. The significant reduction in slump with the addition of nanomaterials is associated with the high reactivity of nanomaterials. nS and nC particles, because of their nano size, provide a substantial increase in available surface area for water adsorption within the fresh mix [11]. It is suggested that, depending on the size of the nanoparticles, they consume some of the free mixing water to promote early C-S-H gels, and occupy much of the micro and nano voids of the cement paste. This leaves an insufficient amount of free water for lubrication between aggregate particles, which unswervingly alters the workable nature and flowability of the concrete. In addition, nS is an active pozzolanic material, where it contributes to the cement hydration process and also helps to promote flocculation in the paste, which, in effect, enhances the stiffness of the fresh concrete matrix [12]. The nC is not as pozzolanic as nS but does help by generating increased nucleation sites for hydration products as well as densifying the binder even at the fresh-laden stage. The high-water demand and subsequently lower slump are a result of the two nanomaterials working synergistically. However, the overall slump value of 51 mm for HSC 3nS 3nC is still an acceptable value for HSC meant for structural elements, for which high workability is not the primary design consideration, but improved density and lower porosity, which enhance mechanical performance and durability, are highly desirable [13].

3.2. Compressive Strength (CS)

The CS of concrete is governed by the structural sturdiness of the bulk cementitious matrix, where the density, continuity, and homogeneity of the C-S-H milieu network determine resistance to uniaxial loading. In the HSC 0nS 0nC control mix, a 28-day robustness of 102.71 MPa was achieved, increasing to 107.32 MPa at 56 days (+4.49%), 112.64 MPa at 90 days (+9.67%), and 115.31 MPa at 180 days (+12.27%). This progressive gain is attributed to the synergistic hydration of OPC with FA and MS. The C₃S and C₂S phases in OPC provide rapid early hydration, forming a dense C-S-H network, while FA contributes to long-term pozzolanic activity, consuming CH and forming additional C-S-H. MS seals capillary pores and refines the ITZ by acting as a pozzolan and ultra-fine filler due to its high surface area and reactivity [14]. By packing in the spaces amongst cement and FA particles, 10% QP increases particle packing density, lowers permeability, and creates a more compact matrix. QS is used as a fine aggregate to ensure optimal gradation and

minimal internal voids. This results in the formation of a rigid granular skeleton that effectively transfers compressive stress. While the SP preserves workability without segregation, the low water-to-cement ratio (0.23) guarantees minimal capillary porosity [15]. In contrast, the HSC 3nS 3nC mix exhibited superior CS development: 113.42 MPa at 28 days, rising to 119.51 MPa at 56 days (+5.37%), 126.93 MPa at 90 days (+11.91%), and 131.68 MPa at 180 days (+16.10%), representing 10.43%, 11.36%, 12.69%, and 14.20% increases over the control mix.

The combined action of nS and nC drives this enhancement, which is not just additive but transformative. By speeding up C-S-H nucleation and consuming CH, nS functions as a highly reactive nucleation site, lowering the volume of reactive phases that are susceptible to chemical attack. Because of its incredibly fine size, it can fill gaps at the nanoscale, obstructing ion diffusion and forming a gel structure that is tightly interlocked [16]. At the same time, nC acts as a hydration catalyst and nano-filler, encouraging early C-S-H nucleation and sub-microscale matrix densification.

A multi-scale pore refinement, from macro to nanoscale, is produced by the combined action of nS and nC, significantly lowering permeability and improving microstructural homogeneity. Additionally, the increased availability of reactive surfaces brought about by nanomaterials amplifies the ongoing pozzolanic activity of FA and MS in the nano-mix, resulting in sustained strength gain that lasts longer than 90 days [17]. This explains the higher percentage increase in strength at later ages, confirming that nanomaterials not only improve early performance but also extend the hydration timeline, making the matrix more durable and resilient under sustained loading. The strength improvements are consistent with prior studies [13], but the long-term gain in this current study is more substantial (14.2% vs 10.5% improvement at 180 days) due to a favourable interaction of the dual nanomaterial. The nano-modified HSC mix used in this research provided a marked improvement in approximately 10% to 14% higher than the traditional HSC mixes with only SCMs (FA and MS), which suggests that nanomaterials supplement the benefits of SCMs but do not necessarily replace those benefits.



Fig. 5 Cylindrical and Prism specimens of HSC

3.3. Split Tensile Strength (STS)

STS is a critical indicator of concrete's resistance to cracking under indirect tensile stress, where failure typically initiates at the ITZ. The HSC 0nS 0nC mix recorded a 28-day STS of 7.96 MPa, increasing to 8.42 MPa at 56 days (+5.78%), 8.93 MPa at 90 days (+12.19%), and 9.01 MPa at 180 days (+13.19%). The ITZ has gradually improved as a result of MS and FA working together to refine it. FA's pozzolanic reaction creates secondary C-S-H, strengthening the bond, while MS's ultra-fine filling of capillary pores in the ITZ decreases microcrack initiation sites. With its angular shape and high surface purity, QS offers excellent mechanical interlock, minimizing debonding under tensile stress, while QP functions as a micro-filler, lowering stress concentrations in the paste [18]. However, the HSC 3nS 3nC mix showed a remarkable improvement in split tensile strength, augmenting from 8.57 MPa at 28 days to 9.15 MPa at 56 days (+6.77%), 9.84 MPa at 90 days (+23.62%), and 9.98 MPa at 180 days (+25.38%), indicating improvements of 7.66%, 8.67%, 10.19%, and 10.77% over the control. The ITZ's nanoscale engineering is principally responsible for this notable improvement. In order to effectively block crack propagation pathways and raise the fracture energy needed for crack initiation, nS enters and fills nanopores in the ITZ. Additionally, it strengthens the interfacial bond by reacting with CH to form dense, low-porosity C-S-H [19]. This is further improved by nC, which forms a stronger, more continuous interfacial layer at the aggregate surface by serving as a gelation site for C-S-H formation. A homogeneous, crack-resistant ITZ is produced by the synergy between nS and nC, delaying the onset of microcracking under splitting loads [20]. Furthermore, the presence of nanomaterials enhances the ongoing pozzolanic activity of FA and MS in the nano-mix, resulting in a quicker densification of the ITZ. QS's uniform gradation guarantees steady load transfer, and the nano-matrix's decreased permeability prevents moisture intrusion, which over time may erode the ITZ. Therefore, the nano-mix's superior split tensile performance is a direct result of interfacial engineering, in which nanomaterials turn the weakest zone into the strongest, rather than merely having a higher compressive strength [21]. Figure 5 shows the specimens cast.

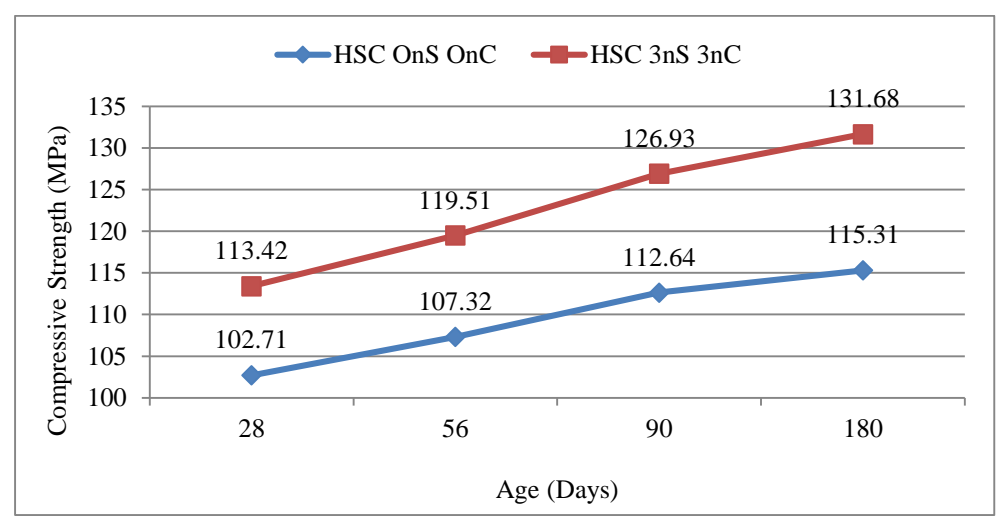


Fig. 6(a) CS of HSC vs Age

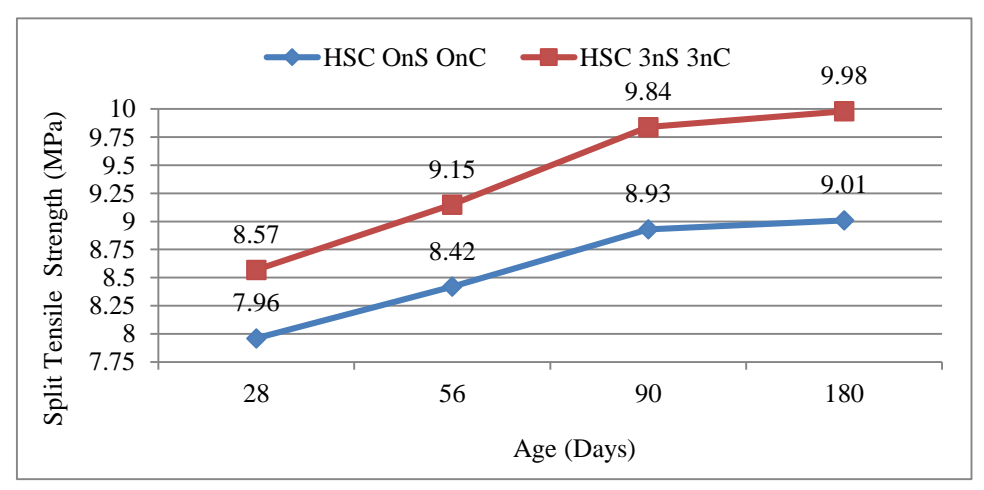


Fig. 6(b) STS of HSC vs Age

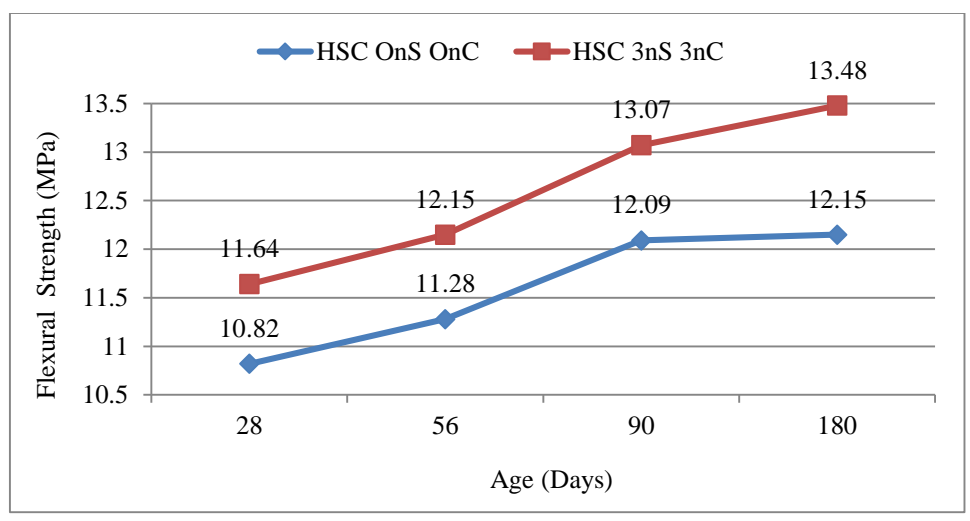


Fig. 6(c) FS of HSC vs Age

3.4. Flexural Strength (FS)

When the bottom fiber of the beam experiences tensile stress and is extremely vulnerable to crack initiation and propagation, the modulus of rupture, or FS, measures the concrete's resistance to bending failure. Flexural performance is more susceptible to post-cracking behavior, ductility, and energy absorption capacity than CS and STS. A 28-day FS of 10.82 MPa was attained by the HSC 0nS 0nC mix, rising to 11.28 MPa at 56 days (+4.25%), 12.09 MPa at 90 days (+11.74%), and 12.15 MPa at 180 days (+12.29%). This improvement results from the matrix's gradual densification brought on by ongoing hydration. Early strength is provided by cement, long-term C-S-H formation is improved by FA, pore structure is refined by MS, and packing density is improved by QP. By ensuring a continuous load path, QS slows the spread of cracks [22, 23]. However, as indicated in Table 3, the HSC 3nS 3nC mix demonstrated remarkable flexural performance: 11.64 MPa at 28 days, increasing to 12.15 MPa at 56 days (+4.38%), 13.07 MPa at 90 days (+12.29%), and 13.48 MPa at 180 days (+15.81%), which correspond to increases of 7.58%, 7.71%, 8.11%, and 10.95%

over the control. The energy-dissipating and crack-bridging mechanisms that nanomaterials introduce are responsible for this significant improvement. As a nano-reinforcement, nS bridges microcracks and stops their growth before they become macrocracks. Its large surface area increases fracture toughness by encouraging a denser, more interconnected C-S-H network. nC improves stress transfer under bending by strengthening the aggregate-paste interface in addition to having a filler effect [24, 25]. A stronger, more ductile matrix that can absorb more energy before failing is produced by the collective accomplishment of nS and nC. The continued hydration of FA and MS further densifies the matrix, reducing flow density, while the well-graded QS ensures uniform stress distribution [26]. The low permeability of the nano-matrix also limits moisture-induced weakening of the tension zone. Therefore, the superior FS of the nano-mix is not just a result of higher CS but a distinct enhancement in fracture mechanics, where nanomaterials improve crack resistance and postcracking behaviour, making the concrete more resilient under bending loads [27]. Figures 6(a), 6(b), and 6(c) are the graphical representations of summaries of CS, STS, and FS.

Table 3. Summary of CS, STS, and FS for HSC Mixes

			HSC 0nS 0nC		HSC 3nS 3nC	
	Age (Days)	Strength (MPa)	% Increase (relative to earlier age)	Strength (MPa)	% Increase (relative to earlier age)	% Increase (w.r.t Control)
	28	102.71	-	113.42	-	10.43
CS	56	107.32	4.49	119.51	5.37	11.36
CS	90	112.64	9.67	126.93	11.91	12.69
	180	115.31	12.27	131.68	16.10	14.20
	28	7.96	-	8.57	-	7.66
STS	56	8.42	5.78	9.15	6.77	8.67
313	90	8.93	12.19	9.84	23.62	10.19
	180	9.01	13.19	9.98	25.38	10.77

	28	10.82	-	11.64	-	7.58
FS	56	11.28	4.25	12.15	4.38	7.71
гъ	90	12.09	11.74	13.07	12.29	8.11
	180	12.15	12.29	13.48	15.81	10.95

3.5. Correlation between CS and STS

STS is an important measure to evaluate resistance to cracking from indirect tensile stress in concrete, particularly in structural members loaded in flexure or from temperature changes. To measure STS is often too resource-intensive; therefore, it will be useful to quantify a reliable empirical relationship with the other concrete property, CS, which is more routinely and reliably measured. In this paper, a power-type equation for predicting STS as a function of CS using regression analysis is developed and substantiated, utilizing a database consisting of control and nano-modified mix as given by equation 1.

The power-law model is used because it can describe the non-linear scaling between CS and ST/FS. RMSE, IAE, NEF, and MAE quantify the mark to which each model fitted the data, with lower RMSE/MAE and higher NEF indicating greater model fit. This power-law model yielded an excellent coefficient of determination ($R^2 = 0.96$), indicating a strong correlation and high predictive accuracy for the tested nanomodified HSC.

The proposed equation is validated against 8 existing models [28-33] from international codes and literature, including IS 456:2000, ACI318-14, etc, and the accuracy of each model is evaluated using statistical performance indicators, including RMSE, IAE, NE, and MAE. As indicated in Table 4, the predicted model is superior to all previous models by producing the lowest RMSE (0.20 MPa), lowest MAE (0.17 MPa), lowest IAE (1.87), and highest NEF (97.8%). Code-based models such as IS 456:2000 and ACI 318-14 are not able to accurately predict the STS of HSC, as

they considerably underestimate the value with RMSE of 1.54 and 2.96 MPa because these models originated from normal-strength concrete databases. The experimental STS values compare favourably with the respective values computed from well-known equations, especially when evaluated alongside empirical models [33].

The flexibility and better fit of the proposed equation result from addressing a non-linear scaling relationship of tensile strength in high-strength, nano-modified concrete. An exponent value of 0.909 suggests that the STS increased based on a corresponding increase in CS, largely due to the influence of nS, nC, MS, FA, and QP contributing to microstructural refinement, which in turn affects the ITZ, reduces porosity, and creates a solid C-S-H gel matrix that is less prone to cracking. The model presented makes predictions with very high accuracy and is a preferred tool for design engineers and researchers working with nano-modified HSC.

With this model, predictions and performances can be made with consistent accuracy, and it is suggested for further use in anticipating tensile performance, quality control, and evaluation of a structural component where resistance to cracking is critical. Table 5 shows the STS predicted values as per different equations, in which Ei is the experimental result, Pi is the proposed STS values, and SP1, SP2, SP3, SP4, SP5, SP6, SP7, and SP8 are the predicted STS values as per various equations (mentioned in Table 4).

$$f_{sts} = 0.119 f_{cs}^{0.909} \tag{1}$$

Where f_{sts} is STS (MPa) and f_{cs} is CS (MPa)

Table 4. S	STS Errors	Based on	Statistical	Metrics
------------	------------	----------	-------------	---------

Ref	Equations	RMSE	IAE	NEF	MAE
Suggested formula	$0.119 f_{cs} 0^{.909}$	0.13	1.24	98.75	0.11
IS 456-2000	$0.7f_{cs}^{0.5}$	1.49	16.06	84.14	1.44
ACI318-14	$0.56 f_{cs}^{0.5}$	2.98	32.85	67.31	2.95
[28]	$0.106 f_{cs}^{0.948}$	0.65	7.06	92.94	0.63
[29]	$0.249 f_{cs}^{0.772}$	0.81	8.86	20.38	0.80
[30]	$0.272 f_{cs}^{0.71}$	1.05	11.45	21.87	7.11
[31]	$0.294 f_{cs}^{0.69}$	1.19	12.98	87.14	1.17
[32]	$0.47 f_{cs}^{0.56}$	2.28	25.03	75.12	2.25
[33]	$0.63 f_{cs}^{0.5}$	1.42	15.46	84.63	1.39

Table 5. STS calculated from different equations

Dorra	М:	CC	STS									
Days	Mix	CS	Ei	Pi	SP1	SP2	SP3	SP4	SP5	SP6	SP7	SP8
28	HSC 0nS 0nC	102.71	7.96	8.02	7.09	5.68	8.56	8.90	7.29	7.18	6.29	6.38
	HSC 3nS 3nC	113.42	8.57	8.78	7.45	5.96	9.40	9.60	7.82	7.69	6.65	6.71

56	HSC 0nS 0nC	107.32	8.42	8.35	7.25	5.80	8.92	9.20	7.52	7.40	6.45	6.53
	HSC 3nS 3nC	119.51	9.15	9.20	7.65	6.12	9.88	10.00	8.12	7.98	6.85	6.89
90	HSC 0nS 0nC	112.64	8.93	8.72	7.43	5.94	9.34	9.55	7.79	7.66	6.62	6.69
	HSC 3nS 3nC	126.93	9.84	9.72	7.89	6.31	10.46	10.47	8.47	8.31	7.08	7.10
180	HSC 0nS 0nC	115.31	9.01	8.91	7.52	6.01	9.55	9.73	7.92	7.78	6.71	6.77
	HSC 3nS 3nC	131.68	9.98	10.05	8.03	6.43	10.83	10.78	8.70	8.53	7.23	7.23

3.6. Correlation between CS and FS

A similar empirical relationship has also been established for CS and FS, with the proposed empirical equation being the one given in Equation 2. Compared to its previous counterpart, this model is exceptional and has an R² of 0.958, which means that it is highly predictive of HSC systems. The proposed equation is compared as well as evaluated with international codes and literature [28,33-36]. Table 6 provides values of RMSE, MAE, IAE, and NEF for the proposed model in comparison with existing models. These outcomes demonstrated that the proposed model provided better results than every existing equation, which is associated with the proposed model having the lowest RMSE (0.17 MPa), lowest MAE (0.13 MPa), lowest IAE (1.07), and highest NEF (98.93%). Code-based models like BS and ACI 318-14, which follow a square-root relationship, show a high overprediction of FS for low CS, and less underprediction for higher CS mainly because those models are developed for normalstrength concrete and did not account for the increased brittleness and microstructural refinement of HSC. With respect to FS, the above proposed power-law models show reasonably well the expected sub-linear scaling of FS with CS. The exponent term of 0.859 shows that, while FS increases with increasing CS, the rate of increase will decrease in the range of higher strength - this phenomenon is attributed to both the increased brittleness and reduced fracture energy of the denser matrices. However, for the HSC 3nS 3nC mix, this scaling trend is offset by the great length of crack-bridging and the nucleation effect of nC and nS, allowing enhanced cohesion within the matrix and interfacial bonding in the tension zone.

Table 7 shows the FS predicted values as per different equations, in which Ei is the experimental result, Pi is the proposed FS values, and FP1, FP2, FP3, FP4, FP5, FP6, and FP7 are the predicted FS values as per various equations (mentioned in Table 6).

$$F_b = 0.203 f_{cs}^{0.859} \tag{2}$$

Where f_b is FS (MPa) and f_{cs} is CS (MPa)

Table 6. FS Errors Based on Statistical Metrics

Ref	Equations	RMSE	IAE	NEF	MAE
Suggested formula	$0.203 f_{cs}^{0.859}$	0.17	1.07	98.93	0.13
IS 456-2000	$0.7f_{cs}^{0.5}$	5.65	46.52	53.59	5.62
ACI318-14	$0.62f_{cs}^{0.5}$	5.44	44.74	55.37	5.41
[28]	$0.034f_{cs}^{1.286}$	3.41	27.50	72.75	3.32
[34]	$0.47f_{cs}^{0.511}$	6.78	55.9	-575.07	6.75
[35]	$0.58f_{cs}^{0.5}$	5.87	48.3	49.37	6.12
[33]	$0.31f_{cs}^{0.7}$	3.46	28.5	71.60	3.44
[36]	$0.0794 f_{cs}^{-1.092}$	2.25	18.3	81.85	2.21

Table 7. FS calculated from different equations

Dorra	Mix	CS	FS									
Days	IVIIX	CS	Ei	Pi	FP1	FP2	FP3	FP4	FP5	FP6	FP7	
28	HSC 0nS 0nC	102.71	10.82	10.85	6.08	6.28	13.13	5.01	5.88	7.93	12.49	
	HSC 3nS 3nC	113.42	11.64	11.82	6.39	6.60	14.92	5.27	6.18	8.50	13.92	
56	HSC 0nS 0nC	107.32	11.28	11.27	6.22	6.42	13.90	5.13	6.01	8.18	13.10	
	HSC 3nS 3nC	119.51	12.15	12.36	6.56	6.78	15.96	5.42	6.34	8.82	14.73	
90	HSC 0nS 0nC	112.64	12.09	11.75	6.37	6.58	14.79	5.25	6.16	8.46	13.81	
	HSC 3nS 3nC	126.93	13.07	13.02	6.76	6.99	17.24	5.58	6.53	9.20	15.74	
180	HSC 0nS 0nC	115.31	12.15	11.99	6.44	6.66	15.24	5.32	6.23	8.60	14.17	
	HSC 3nS 3nC	131.68	13.48	13.43	6.89	7.11	18.08	5.69	6.66	9.44	16.38	

4. Conclusion

This study thoroughly explored the collective governing of nS and nC on the fresh and hardened attributes of M90 grade HSC. The extensive experimental program and subsequent statistical analysis provided the following major conclusions:

- The addition of 3% nS and 3% nC carbonate reduced the slump from 70 mm (control) to 51 mm (nano-modified), indicating that with a high surface area, there was an increased demand for water.
- At 28 days, the CS rose 10.43% (from 102.71 MPa to 113.42 MPa), and it continued to rise until it reached 14.20% at 180 days.
- The STS rose 7.66% at 28 days (from 7.96 MPa to 8.57 MPa) and 10.77% at 180 days.
- FS rose 10.95% at 180 days and 7.58% at 28 days (from 10.82 MPa to 11.64 MPa).
- By enhancing the interfacial bond and facilitating a refined pore structure, the combination of nS and nC created a stronger specimen in every test.
- A strong correlation between CS and STS suggests that the empirical relationship developed can be used to make accurate predictions.

 According to the study, using nano-modification to improve M90 grade HSC's performance for crucial structural applications is an efficient method.

By replacing traditional materials for optimizations, nanomaterials like nS and nC can improve performance efficiency while also potentially lowering the amount of binders in the mixture and promoting sustainability. However, the expense and high energy required for the synthesis of these nanomaterials may prevent their widespread use.

Future research includes studying the life cycle impacts and alternative methodologies to source environmentally friendly nanomaterials from industrial waste streams. The results are valuable in developing dense, durable, and high-performing concrete mixes for structural applications such as high-rise columns, bridge decks, and precast members.

Although it is critical to further investigate durability factors such as chloride permeability, shrinkage, and microstructural characterization with SEM/EDS, this current study only examined mechanical performance under standard curing.

References

- [1] Mounika Ganta, Ramesh Baskar, and Sri Kalyana Rama Jyosyula, "Predicting the Strength Characteristics of Alkali Activated Concrete with Environment Friendly Precursors Using Statistical Methods," *E3S Web of Conferences*, vol. 455, pp. 1-11, 2023. [CrossRef] [Google Scholar] [Publisher Link]
- [2] Qiqi Xu et al., "Experimental Study on Residual Mechanical Properties of Steel-PVA Hybrid Fiber High Performance Concrete after High Temperature," *Construction and Building Materials*, vol. 458, pp. 1-18, 2025. [CrossRef] [Google Scholar] [Publisher Link]
- [3] Hongxuan Tu et al., "Fracture Performance of Ultra High-Performance Concrete (UHPC) at Different Curing Ages: Experimental Investigation and Unified Formulation," *Journal of Sustainable Cement-Based Materials*, vol. 14, no. 9, pp. 1793-1808, 2025. [CrossRef] [Google Scholar] [Publisher Link]
- [4] Shuangquan Qing, and Chuanxi Li, "Mechanical Properties and Microstructure of Low Carbon High-Strength Engineered Cementitious Composites with Supplementary Cementitious Material," *Case Studies in Construction Materials*, vol. 22, pp. 1-20, 2025. [CrossRef] [Google Scholar] [Publisher Link]
- [5] Sumra Yousuf et al., "The Compressive Strength Development and pH of Cement Mortars Incorporating High Volume Supplementary Cementitious Materials under Accelerated Curing," *Heliyon*, vol. 11, no. 3, pp. 1-11, 2025. [Google Scholar] [Publisher Link]
- [6] Naveen Arasu Anbarasu et al., "Pioneering the Next Frontier in Construction with High-Strength Concrete Infused by Nano Materials," *Matéria (Rio de Janeiro)*, vol. 30, pp. 1-14, 2025. [CrossRef] [Google Scholar] [Publisher Link]
- [7] Mohammed Abd El-Salam Arab et al., "Microstructure, Durability and Mechanical Properties of High Strength Geopolymer Concrete Containing Calcinated Nano-Silica Fume/Nano-Alumina Blend," *Construction and Building Materials*, vol. 472, 2025. [CrossRef] [Google Scholar] [Publisher Link]
- [8] Chao Chang et al., "Enhancing Mechanical Properties of High-Strength Recycled Concrete with Basalt Fiber and Nano-Calcium Carbonate: Experimental and Numerical Investigations," *Construction and Building Materials*, vol. 489, pp. 1-25, 2025. [CrossRef] [Google Scholar] [Publisher Link]
- [9] Seyed Sina Mousavi et al., "Influence of Coated Steel Fibers on Mechanical Properties of UHPC Considering Graphene Oxide, Nano-Aluminum Oxide, and Nano-Calcium Carbonate," *Fibers*, vol. 13, no. 4, pp. 1-24, 2025. [CrossRef] [Google Scholar] [Publisher Link]
- [10] Xinkui Yang et al., "Performance Evaluation of Pre-Stressed High-Strength Concrete Pipe Piles Produced with Steel Slag Powder and Ground Quartz sand as Composite Supplementary Cementitious Materials," *Construction and Building Materials*, vol. 478, 2025. [CrossRef] [Google Scholar] [Publisher Link]
- [11] Büşra Aktürk et al., "One-Part Sodium Carbonate-Activated Slag/Calcined Dolomite Mixes: Effects of Nano-Silica on Strength Development, Microstructure and Shrinkage," *Journal of Sustainable Cement-Based Materials*, vol. 14, no. 7, pp. 1293-1309, 2025. [CrossRef] [Google Scholar] [Publisher Link]

- [12] Deprizon Syamsunur et al., "Concrete Performance Attenuation of Mix Nano-SiO2 and Nano-CaCO3 under High Temperature: A Comprehensive Review," *Materials*, vol. 15, no. 20, pp. 1-24, 2022. [CrossRef] [Google Scholar] [Publisher Link]
- [13] Zemei Wu et al., "Mechanisms Underlying the Strength Enhancement of UHPC Modified with Nano-SiO2 and Nano-CaCO3," *Cement and Concrete Composites*, vol. 119, 2021. [CrossRef] [Google Scholar] [Publisher Link]
- [14] Yulius Rief Alkhaly et al., "Characteristics of Reactive Powder Concrete Comprising Synthesized Rice Husk Ash and Quartzite Powder," *Journal of Cleaner Production*, vol. 375, 2022. [CrossRef] [Google Scholar] [Publisher Link]
- [15] Xiao Yang et al., "Study on Workability and Mechanical Strength of Low Cement Ultra-High Performance Concrete with Ultrafine Quartz Powder as Alternative Material under High Temperature Curing," *Case Studies in Construction Materials*, vol. 21, pp. 1-18, 2024. [CrossRef] [Google Scholar] [Publisher Link]
- [16] M.M. Mokhtar et al., "Investigating the Mechanical Performance of Nano Additives Reinforced High-Performance Concrete," *Construction and Building Materials*, vol. 320, 2022. [CrossRef] [Google Scholar] [Publisher Link]
- [17] Zhizhuo Feng et al., "Effect of Nano-CaCO3 on Early-Age Properties and Cracking Potential of High-Strength Concrete," *Journal of Materials in Civil Engineering*, vol. 35, no. 4, pp. 1-13, 2023. [CrossRef] [Google Scholar] [Publisher Link]
- [18] Mavoori Hitesh Kumar et al., "Mechanical Behaviour of High Strength Concrete Modified with Triple Blend of Fly Ash, Silica Fume and Steel Fibers," *Materials Today: Proceedings*, vol. 65, no. 2, pp. 933-942, 2022. [CrossRef] [Google Scholar] [Publisher Link]
- [19] Zhi-hang Wang et al., "Effect of Nano-SiO2 and Nano-CaCO3 on the Static and Dynamic Properties of Concrete," *Scientific Reports*, vol. 12, pp. 1-16, 2022. [CrossRef] [Google Scholar] [Publisher Link]
- [20] Jayaraman Ariyagounder, and Senthilkumar Veerasamy, "Experimental Investigation on the Strength, Durability and Corrosion Properties of Concrete by Partial Replacement of Cement with Nano-SiO2, Nano-CaCO3 and Nano-Ca(OH)2," *Iranian Journal of Science and Technology, Transactions of Civil Engineering*, vol. 46, pp. 201-222, 2022. [CrossRef] [Google Scholar] [Publisher Link]
- [21] Maysam Shmlls, Dávid Bozsaky, and Tamás Horváth, "Compressive, Flexural and Splitting Strength of Fly Ash and Silica Fume Concrete," *Pollack Periodica*, vol. 17, no. 1, pp. 50-55, 2021. [CrossRef] [Google Scholar] [Publisher Link]
- [22] Ramalingam Malathy et al., "Use of Industrial Silica Sand as a Fine Aggregate in Concrete—An Explorative Study," *Buildings*, vol. 12, no. 8, pp. 1-26, 2022. [CrossRef] [Google Scholar] [Publisher Link]
- [23] Xing Xiong et al., "Performance and Microstructure of Ultra-High-Performance Concrete (UHPC) with Silica Fume Replaced by Inert Mineral Powders," *Construction and Building Materials*, vol. 327, 2022. [CrossRef] [Google Scholar] [Publisher Link]
- [24] Musa Adamu et al., "A Soft Computing Technique for Predicting Flexural Strength of Concrete Containing Nano-Silica and Calcium Carbide Residue," *Case Studies in Construction Materials*, vol. 17, pp. 1-15, 2022. [CrossRef] [Google Scholar] [Publisher Link]
- [25] Dejian Shen et al., "Cracking Failure Behavior of High Strength Concrete Containing Nano-CaCO3 at Early Age," *Cement and Concrete Composites*, vol. 139, 2023. [CrossRef] [Google Scholar] [Publisher Link]
- [26] Abdulkader El-Mir, Salem G. Nehme, and Joseph J. Assaad, "Effect of Binder Content and Sand Type on Mechanical Characteristics of Ultra-High Performance Concrete," *Arabian Journal for Science and Engineering*, vol. 47, pp. 13021-13034, 2022. [CrossRef] [Google Scholar] [Publisher Link]
- [27] Sachin Patil, H. Sudarsana Rao, and Vaishali. G. Ghorpade, "The influence of Metakaolin, Silica Fume, Glass Fiber, and Polypropylene Fiber on the Strength Characteristics of High Performance Concrete," *Materials Today: Proceedings*, vol. 80, pp. 577-586, 2023. [CrossRef] [Google Scholar] [Publisher Link]
- [28] Selim Pul, "Experimental Investigation of Tensile Behaviour of High Strength Concrete," *Indian Journal of Engineering & Materials Sciences*, vol. 15, pp. 467-472, 2008. [Google Scholar]
- [29] G. Lavanya, and J. Jegan, "Evaluation of Relationship between Split Tensile Strength and Compressive Strength for Geopolymer Concrete of Varying Grades and Molarity," *International Journal of Applied Engineering Research*, vol. 10, no. 15, pp. 35523-35527, 2015. [Google Scholar] [Publisher Link]
- [30] Nicholas J. Carino, and H.S. Lew, "Re-Examination of the Relation Between Splitting Tensile and Compressive Strength of Normal Weight Concrete," *Journal Proceedings*, vol. 79, no. 3, pp. 214-219, 1982. [CrossRef] [Google Scholar] [Publisher Link]
- [31] Francis A. Oluokun, Edwin G. Burdette, and J. Harold Deatherage, "Splitting Tensile Strength and Compressive Strength Relationships at Early Ages," *Materials Journal*, vol. 88, no. 2, pp. 115-121, 1991. [CrossRef] [Google Scholar] [Publisher Link]
- [32] M.A. Rashid, M.A. Mansur, and P. Paramasivam, "Correlations between Mechanical Properties of High-Strength Concrete," *Journal of Materials in Civil Engineering*, vol. 14, no. 3, 2002. [CrossRef] [Google Scholar] [Publisher Link]
- [33] P.N. Ojha, Brijesh Singh, and Pranay Singh, "Empirical Equations for Prediction of Split Tensile and Flexural Strength of High Strength Concrete Including Effect of Steel Fiber," *International Journal of Research on Engineering Structures and Materials*, vol. 9, no. 1, pp. 95-112, 2023. [CrossRef] [Google Scholar] [Publisher Link]
- [34] Chamroeun Chhorn, Seong Jae Hong, and Seung Woo Lee, "Relationship between Compressive and Tensile Strengths of Roller-Compacted Concrete," *Journal of Traffic and Transportation Engineering (English Edition)*, vol. 5, no. 3, pp. 215-223, 2018. [CrossRef] [Google Scholar] [Publisher Link]

- [35] Mohammad Smadi, and Ezzddeen Migdady, "Properties of High Strength Tuff Lightweight Aggregate Concrete," *Cement and Concrete Composites*, vol. 13, no. 2, pp. 129-135, 1991. [CrossRef] [Google Scholar] [Publisher Link]
- [36] K. Ashwini, and P. Srinivasa Rao, "Evaluation of Correlation between Compressive and Splitting Tensile Strength of Concrete Using Alccofine and Nano Silica," *IOP Conference Series: Materials Science and Engineering, 3rd International Conference on Inventive Research in Material Science and Technology*, Coimbatore, India, vol. 1091, pp. 1-7, 2021. [CrossRef] [Google Scholar] [Publisher Link]